Journal of Nuclear Medicine, published on May 18, 2023 as doi:10.2967/jnumed.123.265592

^{18}F-FDG PET/CT in the Management of Osteosarcoma

Chiwoo Oh[1], Michael W. Bishop[2], Steve Y. Cho[3], Hyung-Jun Im[1,4,5], and Barry L. Shulkin[6]

[1]Department of Applied Bioengineering, Graduate School of Convergence Science and Technology, Seoul National University, Seoul, Republic of Korea; [2]Department of Oncology, St. Jude Children's Research Hospital, Memphis, Tennessee; [3]Nuclear Medicine and Molecular Imaging Section, Department of Radiology, University of Wisconsin School of Medicine and Public Health, Madison, Wisconsin; [4]Department of Molecular Medicine and Biopharmaceutical Sciences, Graduate School of Convergence Science and Technology, Seoul National University, Seoul, Republic of Korea; [5]Cancer Research Institute, Seoul National University, Seoul, Republic of Korea; and [6]Department of Diagnostic Imaging, St. Jude Children's Research Hospital, Memphis, Tennessee

Learning Objectives: On successful completion of this activity, participants should be able to describe (1) the diagnosis and treatment strategy and response criteria of osteosarcoma; (2) the roles of ^{18}F-FDG PET in staging, prediction of clinical outcome and detection of recurrent disease; and (3) the useful timepoint of ^{18}F-FDG PET in prediction of clinical outcome.

Financial Disclosure: Drs. Chiwoo Oh and Hyung-Jun Im were supported by National Research Foundation of Korea (NRF) (NRF-2021M2E8A1039564, 2020R1C1C1009000, and 2019M2D2A1A01058210), Korea Evaluation Institute of Industrial Technology (KEIT) grant funded by the Korea government (MOTIE) (no. 20018522), and Korea Drug Development Fund funded by Ministry of Science and ICT, Ministry of Trade, Industry, and Energy, and Ministry of Health and Welfare (HN22C0632). Dr. Shulkin was supported by the American Lebanese Syrian Associated Charities (ALSAC). Dr. Im is the cofounder and the Chief Scientific Officer of Portrai. The authors of this article have indicated no other relevant relationships that could be perceived as a real or apparent conflict of interest.

CME Credit: SNMMI is accredited by the Accreditation Council for Continuing Medical Education (ACCME) to sponsor continuing education for physicians. SNMMI designates each *JNM* continuing education article for a maximum of 2.0 AMA PRA Category 1 Credits. Physicians should claim only credit commensurate with the extent of their participation in the activity. For CE credit, SAM, and other credit types, participants can access this activity through the SNMMI website (http://www.snmmilearningcenter.org) throsugh June 2026.

Osteosarcoma is the most common type of primary malignant bone tumor. ^{18}F-FDG PET/CT is useful for staging, detecting recurrence, monitoring response to neoadjuvant chemotherapy, and predicting prognosis. Here, we review the clinical aspects of osteosarcoma management and assess the role of ^{18}F-FDG PET/CT, in particular with regard to pediatric and young adult patients.

Key Words: osteosarcoma; ^{18}F-FDG PET; clinical outcome; prediction; staging

J Nucl Med 2023; 00:1–10
DOI: 10.2967/jnumed.123.265592

Osteosarcoma is the most common type of primary malignant bone tumor. ^{18}F-FDG PET/CT is useful for staging, detecting recurrence, monitoring response to neoadjuvant chemotherapy (NCT), and predicting prognosis. Here, we review the clinical aspects of osteosarcoma management and assess the role of ^{18}F-FDG PET/CT, in particular with regard to pediatric and young adult patients.

DEMOGRAPHICS

Osteosarcoma is the most common type of malignant primary bone tumor, with a peak incidence in 10- to 14-y-olds (*1*) and a second peak incidence in those older than 50 y. Approximately 4.4 cases per million are diagnosed annually in people aged 0–24 y (*2*). Primary osteosarcomas commonly arise within the metaphyses of long bones, with 80% presenting within an extremity. Patients typically present with pain that progresses over weeks to months, with localized swelling and a diminished range of motion or function in the affected limb (*3*). At the time of diagnosis, approximately 10%–20% of patients have evidence of macroscopic metastasis, most commonly in the lung (81%), bone (34%), and, rarely, lymph nodes (2%) (*4*). Five-year event-free survival rates are approximately 70% (*5*). ^{18}F-FDG PET/CT has multiple roles in the evaluation of osteosarcoma for staging, clinical and histologic response to therapy during and at the conclusion of treatment, and determining prognosis after completion of therapy (Fig. 1).

STAGING

^{18}F-FDG PET/CT is useful for staging, detecting recurrence, and predicting histologic response and prognosis in the investigation of osteosarcoma. Conventional imaging modalities other than ^{18}F-FDG PET/CT for staging osteosarcoma are summarized in Supplemental Figure 1 (supplemental materials are available at http://jnm.snmjournals.org). During staging, PET/CT is useful for differential diagnosis of primary bone neoplasms and detecting metastatic lesions (Figs. 2 and 3; images are scaled to SUV units as on the color and intensity bars). Combining PET imaging with CT or MRI provides more accurate information on the staging of osteosarcoma than is possible with PET imaging alone (*6,7*). Also, whole-body imaging with PET/CT can be helpful in staging because osteosarcoma favors the extremities and can be widely metastatic (*8*). London et al. retrospectively compared the sensitivity and specificity of PET/CT and plain radiography for detecting malignant lesions, including primary and metastatic disease, in patients with pediatric primary bone tumors. PET/CT was more sensitive than plain radiography (98% vs. 83%) and more specific (97% vs. 78%) (*9*). Strobel et al. compared the diagnostic accuracy of plain radiography, PET, and PET/CT. They found that PET/CT showed 95% sensitivity and 77% specificity, which were the highest rates

Received Feb. 15, 2023; revision accepted Apr. 26, 2023.
For correspondence or reprints, contact Hyung-Jun Im (iiihjjj@gmail.com) or Barry L. Shulkin (barry.shulkin@stjude.org).
Published online May. 18, 2023.

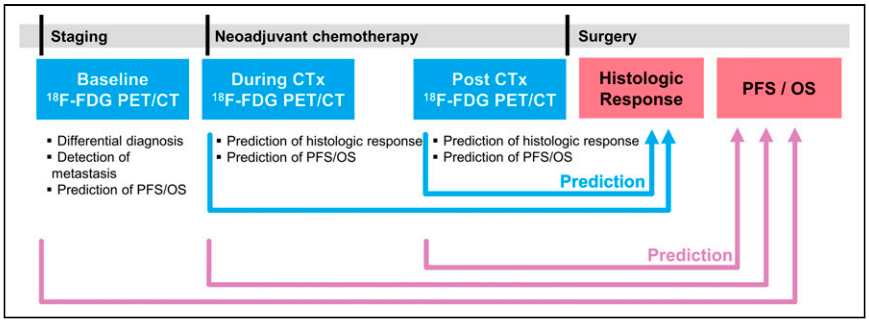

FIGURE 1. Role of ^{18}F-FDG PET/CT in staging and outcome prediction in osteosarcoma. CTx = chemotherapy; PFS = progression-free survival.

among the imaging modalities (*10*). Quartuccio et al. reported that PET/CT has higher accuracy for detecting bone metastasis than CT or dedicated MRI and detects lung metastasis as well as CT does (*11*). Franzius et al. found that PET performed better than bone scanning for detecting bone metastasis (*12*), with Hurley et al. finding that PET/CT was more sensitive but bone scanning was more specific (*13*). Used together in a lesion-based analysis (*14*), the sensitivity of PET/CT plus bone scanning was 100%, which is higher than that of PET/CT or bone scanning alone, supporting the use of both modalities together to detect bone metastasis (Table 1). This is because some osteoblastic metastases may not show elevated uptake of ^{18}F-FDG, thus yielding false-negative results on PET/CT but positive results on bone scanning (*14*). In our experience, false-negative cases are rare, and careful review of the CT bone window in a PET/CT scan could reduce them. Thus, we do not routinely perform bone scans on patients with osteosarcoma.

In a recent metaanalysis, the value of PET/CT in diagnosis and staging was summarized (*15*). This metaanalysis evaluated 26 studies, including the above-mentioned studies. For detecting primary lesions, PET/CT showed 100% sensitivity in 14 studies. Pooled sensitivity and specificity for detecting lung metastases in 8 studies were 81% (95% CI of 72%–88%) and 94% (95% CI of 89%–97%), respectively. For bone metastases, 6 studies showed a pooled sensitivity of 93% (95% CI of 87%–97%) and a pooled specificity of 97% (95% CI of 96%–98%) (Supplemental Fig. 2). Thus, PET/CT is useful for differential diagnosis of the suspected primary bone lesions and for staging.

TREATMENT OVERVIEW

The therapeutic standard of care involves NCT with 3 or more agents with single-agent activity for approximately 8–10 wk, followed by surgical resection of all detectable disease (including metastases) and postoperative adjuvant chemotherapy for 12–29 wk (*16*). Limb-salvage surgery is the surgical treatment in 85%–90% of patients with osteosarcoma, providing better functional and cosmetic results than amputation without compromising survival (*17*).

PREDICTION OF RESPONSE TO NCT

Histologic Response

In 1994, a critical appraisal of osteosarcoma prognostic factors concluded that the histologic response of primary tumors after NCT is the most significant factor in predicting disease-free survival (*3,18*). Although histologic response is prognostic for outcomes, dose-intensifying NCT to increase rates of tumor necrosis have not yielded superior survival curves (*19*). Similarly, adding chemotherapeutic agents for patients experiencing a poor response has not improved their event-free survival or overall survival (OS) (*19*). Several grading systems for assessing the effect of NCT on the primary tumor indicate that having at least 90% tumor necrosis after NCT is a favorable response (Table 2) (*20–22*).

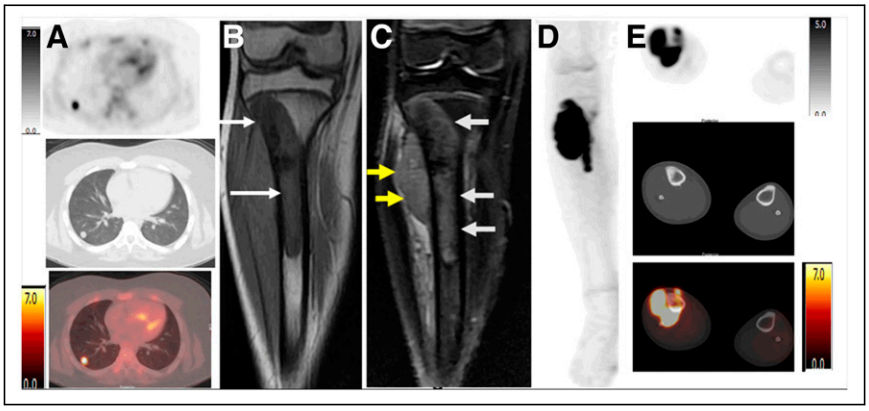

FIGURE 2. A 13-y-old boy with right leg pain. (A) ^{18}F-FDG PET CT shows 1-cm nodule with markedly elevated uptake in right lower lobe (SUV_{max}, 6.7) (^{18}F-FDG PET emission image [top], CT transmission image [middle], and PET/CT image [bottom]). (B) Hypointense signal on coronal T1 MR image shows tumor extending from tibial metaphysis through proximal third of right tibia (arrows). (C) Coronal T2 short-tau inversion recovery MR image shows intermediate signal within intramedullary component of tumor (white arrows), corresponding to hypointense T1 signal, and hyperintensity in soft-tissue component lateral to tibia (yellow arrows). (D) ^{18}F-FDG PET/CT anterior maximum-intensity-projection view shows intense uptake in the proximal aspect of the right distal lower extremity. (E) ^{18}F-FDG PET axial emission image (top), transmission CT bone window (middle), and PET/CT image (bottom) show intense though irregularly increased uptake of ^{18}F-FDG in both bone and soft-tissue components of tumor (SUV_{max}, 15.^{TM}).

Role of ^{18}F-FDG PET/CT

In osteosarcoma, the ability of PET or PET/CT to predict histologic response during or after NCT has been reported. In 1996, Jones et al. first reported using PET to assess response to NCT in 3 patients with osteosarcoma (*23*), finding that SUV declined after NCT, which reflected the histologic response. In the following studies, tumor-to-background ratio or SUV_{max} after NCT, as well as tumor-to-background ratio or SUV_{max} ratio between PET at baseline and after NCT, were found to predict histologic response (*23–32*). Meanwhile, some studies reported that PET/CT was not predictive of histologic response (Table 3; Supplemental Table 1) (*33,34*). These studies agree on the following optimal cutoffs of PET parameters: an SUV_{max} of 2–3 after NCT and a tumor-to-background ratio or SUV_{max} ratio of 0.4–0.6 (*24–29,31–33,35–38*). In a metaanalysis, an SUV_{max} after NCT of less than 2.5 and an SUV_{max} ratio of less than 0.5

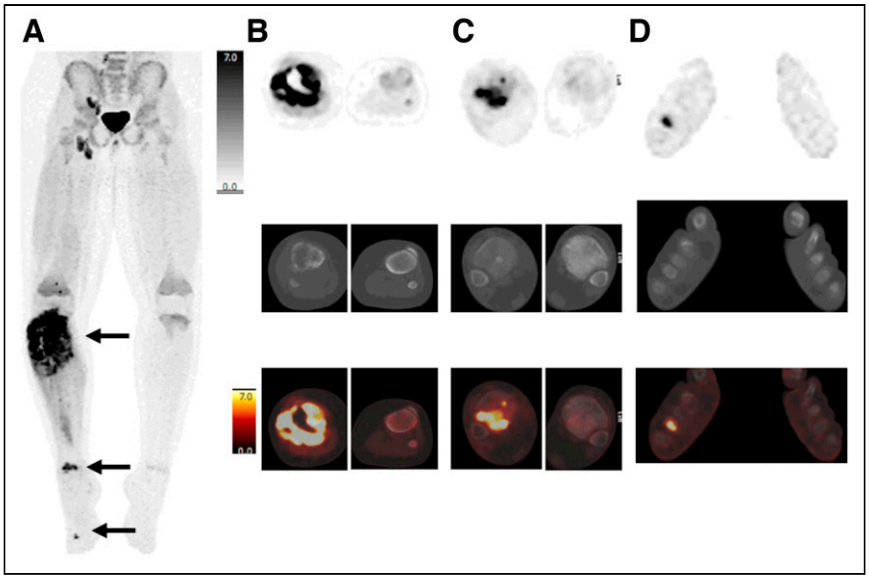

FIGURE 3. A 10-y-old girl with pain in right lower extremity. (A) Anterior maximum-intensity-projection PET image shows primary tumor in proximal right tibia and soft tissue (top arrow; SUV_{max}, 24.4), unsuspected site of metastatic disease in distal right tibia (middle arrow; SUV_{max}, 12.9), and unsuspected site of metastatic disease in fourth right metatarsal (bottom arrow; SUV_{max}, 8.2). (B–D) PET (top), CT (middle), and PET/CT fusion (bottom) images showing the sites indicated in A by top arrow (B), middle arrow (C), and bottom arrow (D). Uptake in ipsilateral popliteal, inguinal femoral, and iliac lymph nodes was considered reactive.

between baseline and after NCT were suggested as optimal cutoffs (*39*). Because of the ability of PET/CT to predict the histologic response, Harrison et al. have proposed further evaluating PET/CT as an imaging biomarker to screen the potential of targeted agents in osteosarcoma (*40*).

Predicting the histologic response of tumor during NCT may be a better option than doing so after completion of NCT in the clinic because the latter is too late to modify the NCT regimen. In 2012, Im et al. found that SUV_{max} after 1 cycle of NCT can also predict the histologic response with an accuracy of 92.9% using a cutoff of 3.2 (*37*). This result was reproduced by Byun et al. in 2014 (*41*) and Davis et al. in 2018 (*38*). Metabolic–volumetric parameters of PET, such as metabolic tumor volume (MTV) and total lesion glycolysis (TLG, the product of tumor segmented SUV_{mean} and MTV), during and after the NCT also showed predictive value for histologic response (*36,37,41*). Byun et al. reported that SUV_{max}, MTV, and TLG after 1 cycle of NCT could predict histologic response, but tumor volume assessed by MRI could not (*41*). Among PET parameters, SUV_{max} could be a better choice than metabolic–volumetric parameters because MTV and TLG measurements depend on the PET tumor segmentation methods, which are not standardized (*42*). Also, SUV_{max} during NCT performed similarly to MTV and TLG in predicting the histologic response (area under the curve, 0.956 for all parameters) (*37*). Because the level of water molecule diffusion can be changed according to the cellularity of the primary lesion, diffusion-weighted MRI can be used to predict the histologic response of osteosarcoma; thus, combining PET and diffusion-weighted MRI may be an effective method to predict the histologic response (*35*).

Furthermore, predicting tumor histologic response using the baseline PET/CT has been attempted. Byun et al. used dual-phase (i.e., dual-time point) baseline PET/CT obtained at 60 and 120 min after ^{18}F-FDG injection (*43*), finding that the mean retention index at baseline PET/CT was predictive of histologic response, with a moderate accuracy of 71% (Supplemental Fig. 3). However, Im et al. reported that although conventional parameters of baseline PET/CT could not predict histologic response, kurtosis and skewness among histogram-based parameters could, with areas under the curve of 0.718 and 0.714, respectively. The predictive value could be enhanced using a machine learning algorithm (area under the curve, 0.821), but the predictive values of texture features depended on the type of segmentation method and machine learning algorithm (*44*). Altogether, more evidence is needed to prove that baseline PET/CT is predictive of histologic response after NCT.

PREDICTION OF OUTCOMES

Prognostic Factors

Tumor site, size, primary metastases, response to chemotherapy, and surgical remission are the reported independent prognostic factors in osteosarcoma (*3*). Osteosarcoma arising in pelvic or axial bones has a worse prognosis than that of disease in extremity bones, with pelvic osteosarcoma having reported 5-y OS rates of 27%–47% (*45*). Osteosarcoma arising in the spine has an even worse prognosis, with a median survival time of 10–23 mo (*46*). Tumor stage is also prognostic. In the Musculoskeletal Tumor Society's Enneking system, stage IA showed an almost 100% 5-y survival rate, yet IIB showed a 5-y survival rate of only 40% (*47*). Among patients with metastases, those with only lung metastases have a more favorable prognosis than do those with extrapulmonary lesions (5-y OS rate, 38% vs. 10.9%) (*3*). The presence of skip metastasis is associated with a poor prognosis (*48*). Being younger than 40 y is a good prognostic factor (5-y survival rate, 65.1% vs. 55.0%) (*3*). In the literature, the most reliable cutoff differentiating favorable from unfavorable response to chemotherapy is 90% necrosis, with greater than 90% necrosis considered favorable (*31*). Prognostic factors can be applied differently according to age. Response to chemotherapy is applied as a prognostic factor in pediatric patients but not in adult patients (*49*). Meanwhile, pathologic fracture was associated with poor prognosis in adult patients but not in pediatric patients (*50*).

Role of ^{18}F-FDG PET/CT

Evaluations of the prognostic value of PET/CT parameters are summarized in Table 4. In 2009, Costelloe et al. was the first to report that SUV_{max} and TLG, both at baseline and after NCT, could predict progression-free survival and OS (*51*). Hawkins et al. reported that an SUV_{max} of over 2.5 after NCT is associated with worse progression-free survival (*33*). Byun et al. also reported that baseline MTV and TLG could predict metastasis-free survival (*52*). However, Bailly et al.'s tests of multiple baseline PET/CT parameters for predicting prognosis indicated that only the elongation feature, a type of shape feature, was significantly associated with progression-free survival and OS (*53*). The elongation feature is the ratio of the longer and shorter edges of the smallest rectangle that encloses the measured region. An elongation factor of 1 indicates maximum symmetry. Most PET/CT parameters were not

TABLE 1
Staging and Diagnosis using ^{18}F-FDG PET/CT vs. Other Imaging Modalities

Objective	Study design	Patients (*n*)	Age (y) Median	Age (y) Mean	Procedure	Category	Sensitivity	Specificity	Accuracy	Reference
Differential diagnosis of primary lesion	Prospective	50	NR	36.9	Conventional radiograph		85%	65%	78%	(*10*)
					PET		85%	35%	68%	
					PET/CT		91%	77%	86%	
Detection of lung metastasis	Retrospective	20	NR	13.1	PET/CT		84%	79%	95%	(*11*)
					CT		94%	71%	67%	
Detection of bone metastases	Retrospective	70	14	NR	PET	Patient	90%	96%	95%	(*12*)
						Lesion	72%	NR	NR	
					BS	Patient	71%	92%	88%	
						Lesion	72%	NR	NR	
Detection of bone metastases	Retrospective	206	15	NR	PET/CT	Patient	94.5%	98.1%	98%	(*14*)
						Lesion	92.1%	NR	NR	
					BS	Patient	76.3%	97.0%	97%	
						Lesion	74.2%	NR	NR	
					PET/CT + BS	Patient	100%	96.3%	97%	
						Lesion	100%	NR	NR	
Detection of bone metastases	Retrospective	39	12	NR	PET/CT		95%	98%	98%	(*13*)
					BS		76%	97%	96%	
					PET/CT + BS		100%	96%	97%	

NR = not reported; PET = ^{18}F-FDG PET; BS = bone scan.

TABLE 2
Histologic Response Grading Systems

System	Grade	Description
Rosen et al. (*20*)		
	IV	No viable tumor cells
	III	>90% tumor necrosis
	II	50% ≤ 90% tumor necrosis
	I	0% < 50% tumor necrosis
Picci et al. (*21*)		
	Total response	No viable tumor
	Good response	90%∼99% necrosis
	Fair response	60%∼89% necrosis
	Poor response	<60% necrosis
Salzer-Kuntschik et al. (*22*)		
	I	No viable tumor cell
	II	Single tumor cell or 1 vital cell cluster < 0.5 cm
	III	Vital tumor < 10%
	IV	Vital tumor 10%–50%
	V	Vital tumor > 50%
	VI	No effect of chemotherapy

TABLE 3
Predicting Histologic Response Using ^{18}F-FDG PET/CT

Study design	Patients (*n*)	Median age (y)	PET parameter	Time point	Histologic assessment	Histologic responder criteria	Cutoff for histologic responder	Histologic response predicted?	Reference
Prospective	15	17	SUV_{max}, SUV_{max} ratio, TBR, TBR ratio	Baseline, after NCT	Salzer-Kuntschik	Grade I–III (>90% necrosis)	TBR ratio > 0.46	Yes	(*32*)
Prospective	70	14	SUV_{max}, SUV_{max} ratio	Baseline, after NCT	Rosen	Grade III–IV (>90% necrosis)	SUV_{max} (after NCT) ≤ 2, SUV_{max} ratio ≥ 0.6	Yes	(*25*)
Retrospective	40	15.1	SUV_{max}, SUV_{max} ratio	Baseline, after NCT	Salzer-Kuntschik	Grade I–III (>90% necrosis)	SUV_{max} (after NCT) < 2.5, SUV_{max} ratio < 0.5	No	(*33*)
Retrospective	19	24.1	SUV_{max}, SUV_{max} ratio, SUV_{mean}, SUV_{mean} ratio, MTV, MTV ratio	During NCT, after NCT	% necrosis	>90% necrosis	SUV_{max} (after NCT) < 2.5, MTV ratio < 0.5	Yes	(*36*)
Prospective	9	23	SUV_{peak}, SUV_{mean}	Baseline, during NCT, after NCT	% necrosis	NR	NR	Yes	(*23*)
Prospective	27	17	TBR, TBR ratio	Baseline, after NCT	Salzer-Kuntschik	Grade I–III (>90% necrosis)	TBR ratio > 0.6	Yes	(*31*)
Retrospective	16	NR	Visual assessment, TBR, TBR % change	Baseline, after NCT	% necrosis	>90% necrosis	TBR (after NCT) < 1.4	Yes	(*30*)
Prospective	10	18	SUV_{mean}, SUV_{mean} % change	Baseline, after NCT	Salzer-Kuntschik	Grade I–III (>90% necrosis)	NR	No	(*34*)
Retrospective	11	17	SUV_{max}, SUV_{max} ratio	Baseline, after NCT	European Osteosarcoma Intergroup trials	>90% necrosis	SUV_{max} (after NCT) < 2.5, SUV_{max} ratio > 0.5	Yes	(*27*)
Prospective	20	15	SUV_{max}, SUV_{max} ratio, MTV, MTV ratio, TLG, TLG ratio	Baseline, during NCT, after NCT	Salzer-Kuntschik	Grade I–III (>90% necrosis)	SUV_{max} (after NCT) < 3, SUV_{max} (during NCT) < 3.2, SUV_{max} ratio (baseline/during) < 0.49, SUV_{max} ratio (baseline/after) < 0.56	Yes	(*37*)
Prospective	27	15	SUV_{max}, MRV, apparent diffusion coefficient	Baseline, after NCT	Rosen	Grade III–IV (>90% necrosis)	SUV_{max} % change ≥ 52%, apparent diffusion coefficient % change > 13%	Yes	(*35*)
Prospective	31	15	RI_{max}, RI_{mean}	Baseline, after NCT	Rosen	Grade III–IV (>90% necrosis)	RI_{mean} (before NCT) < 10%	Yes	(*43*)

TBR = tumor to background ratio; NR = not reported; RI_{max} = maximum retention index; RI_{mean} = mean retention index.

TABLE 4
Predicting Prognosis Via ^{18}F-FDG PET/CT

Study design	Patients (*n*)	Median age (y)	Time points	Parameters	Clinical outcome	Cutoff for worse prognosis	Hazard ratio	95% CI	*P*	Reference
Retrospective study	31	27.5	Baseline, after NCT	SUV_{max}, TLG	PFS	SUV_{max} (baseline) > 15	4.514	1.335–15.26	0.015	(*51*)
						SUV_{max} (after NCT) > 5	4.527	1.548–13.24	0.006	
						TLG % change (10%)	1.096	1.017–1.181	0.016	
					OS	SUV_{max} (after NCT) > 3.3	NR		0.043	
						TLG (baseline, per unit)	1.003	1.000–1.005	0.021	
Retrospective review	40	15.1	Baseline, after NCT	SUV_{max}	PFS	SUV_{max} (after NCT) > 2.5	NR		0.021	(*33*)
Retrospective study	83	16	Baseline, after NCT	SUV_{max}, MRV, MTV, TLG	Metastasis-free survival	Baseline MTV (2.0) > 105	3.8	1.5–9.59	0.002	(*52*)
						Baseline TLG (45%) > 187	2.47	1.056–5.79	0.037	
Retrospective study	31	13.9	Baseline, after NCT	SUV_{max}, SUV_{peak}, SUV_{mean}, MTV, TLG, textural features, shape features	PFS	Elongation (baseline) (cutoff NR)	5.583	NR	0.019	(*53*)
					OS	Elongation (baseline) (cutoff NR)	7.113	NR	0.0062	
Retrospective review	34	12.2	Baseline, during NCT, after NCT	SUV_{max}, SUV_{peak}, MTV, TLG	Event-free survival	MTV (2.5) (baseline) > 238.06	5.024*	1.51–16.77	0.01*	(*54*)
						TLG (2.5) (baseline) > 981.97	5.740*	1.34–24.51	0.006*	
						MTV (2.5) (during NCT) > 35.8	8.155*	1.52–43.69	0.046*	
					OS	MTV (2.5) (baseline) > 238.06	29.447*	2.21–392.27	0.033*	
						TLG (2.5) (baseline) > 1,022.3	29.447*	2.21–392.27	0.033*	
						TLG (2.5) (during NCT) > 120.4	34.789*	2.50–483.84	0.033*	

Retrospective review = retrospective review of prospective study; PFS = progression-free survival; NR = not reported.

*Adjusted for histologic response.

Numbers in parentheses indicate segmentation methods to measure MTV and TLG, with (2.0) indicating fixed absolute threshold of SUV 2.0, (2.5) indicating fixed absolute threshold of SUV 2.5, and (45%) indicating fixed relative threshold of 45% of SUV_{max}.

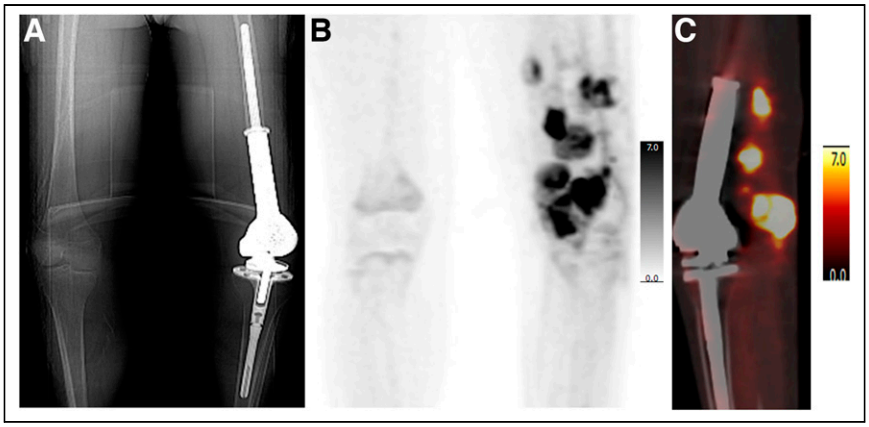

FIGURE 4. A 15-y-old boy with history of osteosarcoma in left femur and limb-sparing procedure on left lower extremity. (A) Topogram from attenuation-correction CT shows rotating-hinge modular prosthesis in left distal femur and left knee. (B) Anterior maximum-intensity projections shows multiple areas of markedly elevated uptake in left lower extremity. (C) PET/CT sagittal view of left leg shows numerous soft-tissue nodules with intense uptake posterior to prosthesis (SUV_{max}, 20.3).

prognostic in the study, and the parameters were used as continuous variables only. However, the previous studies found that the dichotomized PET/CT parameters are prognostic (*53*). We reported that most of the dichotomized PET/CT parameters, including SUV_{max}, SUV_{peak}, MTV, and TLG at baseline, during, and after NCT, are predictive of event-free survival and OS (Supplemental Fig. 4). Furthermore, we found that the parameters were predictive of event-free survival and OS even after adjustment for the histologic response and initial staging (*54*).

The studies showed similar results via diverse methods. For example, the segmentation methods of MTV and TLG vary widely. Costelloe et al. set a relative SUV threshold of 45% (*51*), but Byun et al. used fixed SUV thresholds of 2%, 2.5%, and 45% (*52*). Im et al. used the fixed SUV thresholds of 2% and 2.5%, relative SUV thresholds of 40% and 60%, and liver-based thresholds, reporting that fixed thresholds or liver-based thresholds were more robust than relative thresholds in predicting prognosis. The MTV and TLG based on relative thresholds were not prognostic during or after NCT because the tumor volumes tend to be overestimated (*54*). Also, the cutoffs of parameters for predicting prognosis differed: Hawkins et al. used the an SUV_{max} cutoff of 2.5 (*33*); the other studies used the optimized cutoffs (*51,52,54*). All studies were retrospective in some way, necessitating larger, prospective studies to confirm these results and to define the optimal cutoff for predicting prognosis in osteosarcoma.

RECURRENT DISEASE

PET/CT can detect osteosarcoma recurrence after completion of treatment (Fig. 4; Supplemental Fig. 5). A metaanalysis of the detection of recurrent disease in 7 studies revealed excellent diagnostic performance, with pooled sensitivity and specificity rates of 91% (95% CI, 81% to 96%) and 93% (95% CI, 87% to 97%), respectively (*15*). Angelini et al. assessed the diagnostic accuracy of PET/CT for detecting recurrence in 37 patients who were treated with adequate surgical resection, were suspected to have relapsed disease, and had histologic validation of disease relapse after PET/CT. Altogether, 33 patients (89.2%) had PET/CT-detected recurrence. The sensitivity, specificity, and accuracy were 91%, 75%, and 89%, respectively (*55*). Likewise, Sharp et al. reported that PET/CT was positive in 10 local recurrences, observing either a solid or a peripheral/nodular pattern with a wide range of SUV_{max} (3.0–15.7) (*56*). Osteosarcoma has the potential to metastasize to various organs; examples of such metastases include cerebral (Fig. 5), pulmonary pleural caking (Supplemental Fig. 6), epimyocardial (Supplemental Fig. 7), renal (Fig. 6), pancreatic (Supplemental Fig. 8), and tumor thrombosis (Supplemental Fig. 9).

PET/MRI

Generally, PET/MRI has advantages over PET/CT for its excellent soft-tissue contrast and lower radiation exposure, which is a clear benefit for pediatric patients (*57,58*). Schäfer reported that PET/MRI showed a 73% reduction in radiation exposure compared with PET/CT and demonstrated an identical rate of detecting lesions (*59*). Platzek et al. reported that TNM staging of PET/MRI was almost identical to that of conventional modalities (CT plus MRI) in 29 patients with sarcoma (*60*). Also, Eiber et al. compared the ability of PET/MRI and PET/CT to detect bone metastasis in patients with various primary malignancies. They reported that PET with T1-weighted turbo spin echo MRI did not provide a significant difference in detection of malignant bone lesions but was superior to PET/CT in the anatomic delineation of ^{18}F-FDG-positive lesions (*61*). Buchbender et al. suggested in their continuing education paper that PET/MRI could provide similar diagnostic accuracy for T staging with MRI alone and similar performance for N staging with PET/CT. (*62*). Orsatti et al. found that in 13 pediatric sarcoma patients, there was a significant negative correlation between apparent diffusion coefficients and SUV in primary lesions as measured using PET/MRI (*63*). In response monitoring, whole-body diffusion-weighted MRI during induction chemotherapy could predict

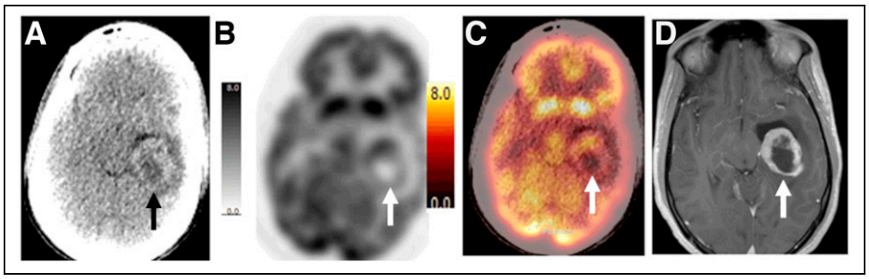

FIGURE 5. A 23-y-old man with progressive metastatic osteosarcoma: attenuation-correction CT image (A), PET emission image (B), PET/CT image (C), and axial T1 MR image (D). ^{18}F-FDG PET/CT shows previously unknown left temporal lobe metastasis (arrows) (SUV_{max}, 6.4). There is uptake at periphery of lesion, with reduced uptake centrally, consistent with necrosis. Contrast-enhanced T1 MR image obtained following day shows irregularly rimmed ring enhancing lesion in left temporal lobe, consistent with metastatic disease.

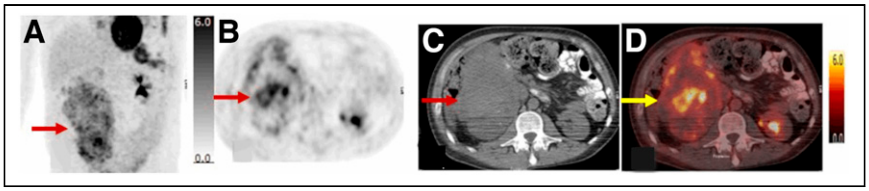

FIGURE 6. A 25-y-old man with multiple recurrent osteosarcoma and large right renal metastasis (arrows; SUV_{max}, 7.1): anterior maximum-intensity-projection view (A); ^{18}F-FDG PET axial emission image (B), corresponding axial CT image from attenuation correction lesion localization CT (C), and PET/CT image (D).

clinical response well (area under the curve, 0.98) and exhibited significant agreement with PET/MRI in 56 patients with sarcoma or lymphoma. The biologic and clinical significance of discordant response assessment between diffusion-weighted MRI and PET/MRI in 8 of the 56 patients has not been assessed (*64*). Therefore, it is warranted to evaluate the additive value by combination of PET/MRI with diffusion-weighted MRI in response monitoring. In addition, Baratto et al. described that PET/MRI can improve monitoring of response to immunotherapy and potentially be used for identification of nonresponders by tumor-associated macrophage imaging using iron oxide nanoparticles (*65*).

NEW TRACERS

^{18}F-NaF is an excellent bone-seeking agent; therefore, NaF PET has been used for skeletal imaging for many decades (*66*). Pathologic bone changes and soft-tissue metastasis with dystrophic calcification can be detected by NaF PET (*67*). Cai et al. reported that NaF PET images could detect hepatic metastasis in patients with osteosarcoma. ^{18}F-NaF activity was more prominent in the calcified lateral portion (*68*). Chou et al. reported that ^{18}F-NaF could detect cardiac osteosarcoma metastasis, which is a rare metastatic site in patients with osteosarcoma (*67*). Also, Verma et al. reported that NaF PET could detect a tumor thrombus arising from osteosarcoma (*69*). Recently, Kairemo et al. proposed NaF PET-based response criteria: NaF PET response criteria for solid tumors (NAFCIST). In the study, the treatment response of 17 patients with metastatic osteosarcoma who were treated with $^{223}RaCl_2$ was assessed using conventional PERCIST based on ^{18}F-FDG PET/CT and NAFCIST based on NaF PET. NAFCIST could predict the OS but PERCIST could not (*70*). Altogether, NaF PET is excellent for finding specific tumor regions, including rare metastasis, and could be a good prognostic biomarker.

Radiolabeled fibroblast activation protein inhibitors (FAPIs) have attracted increasing attention as new theranostic agents that specifically target cancer-associated fibroblast (*71–73*). Kratochwil et al. retrospectively evaluated ^{68}Ga-FAPI PET uptake in 80 patients with 28 different types of malignancies, including 8 patients with sarcoma. The SUV_{mean} of the sarcoma group was the second highest among 28 types of malignancies (*71*). Koerber et al. retrospectively evaluated the diagnostic ability of ^{68}Ga-FAPI PET in 15 patients with sarcoma, including 1 with osteosarcoma. ^{68}Ga-FAPI PET showed high potential as a probe for diagnosis in sarcoma because it showed high uptake in the primary tumor (median, 7.16; range, 4.64–9.79) (*72*). Kessler et al. compared the accuracy of ^{68}Ga-FAPI PET with that of ^{18}F-FDG PET in 47 patients with sarcoma, including 8 patients with osteosarcoma. They found a significant association between FAP expression and ^{68}Ga-FAPI PET uptake through histopathologic verification (Spearman r = 0.43, P = 0.03). In per-patient basis analysis, the detection rate of ^{68}Ga-FAPI and ^{18}F-FDG PET were 76.6% and 81.4%, respectively. However, ^{68}Ga-FAPI PET could detect more metastatic lesions, resulting in an upstaging compared with ^{18}F-FDG PET in 8 (18.6%) patients (*73*). On the basis of the promising results in these early imaging studies of FAPI PET in patients with sarcoma, further studies are warranted to compare the performance of FAPI PET in various clinical situations, such as staging, treatment monitoring, and recurrence, with that of current standard imaging modalities, including ^{18}F-FDG PET. Furthermore, a theranostic approach using FAPI could open new avenues for osteosarcoma management (*74*).

The membrane glycolipid GD2 is overexpressed in osteosarcoma; however, anti-GD2 immunotherapy for recurrent osteosarcoma has been limited because of the intertumoral heterogeneity of GD2 expression in osteosarcoma. Therefore, immuno-PET agents to assess GD2 expression have been developed and have shown promising results in a preclinical PET/CT study (*75*) and a PET/MRI case report of an osteosarcoma patient with lung metastasis (*76*).

CONCLUSION

In osteosarcoma, ^{18}F-FDG PET/CT is useful for staging, monitoring response to therapy, predicting prognosis, and characterizing recurrent disease. It has been extensively validated in studies involving pediatric patients, and similar findings have also been observed in research that includes adult patients, highlighting its effectiveness across different age groups. ^{18}F-FDG PET/CT could ease the drug development process for newer osteosarcoma therapies by facilitating patient selection based on prognosis and serving as early determinants of disease response.

ACKNOWLEDGMENTS

We thank Cherise Guess, PhD, ELS, senior scientific editor, St. Jude Children's Hospital, for expert review and advice, and Amanda Meek for expert administrative support.

REFERENCES

1. Kansara M, Teng MW, Smyth MJ, Thomas DM. Translational biology of osteosarcoma. *Nat Rev Cancer.* 2014;14:722–735.
2. Mirabello L, Troisi RJ, Savage SA. Osteosarcoma incidence and survival rates from 1973 to 2004: data from the Surveillance, Epidemiology, and End Results Program. *Cancer.* 2009;115:1531–1543.
3. Bielack SS, Kempf-Bielack B, Delling G, et al. Prognostic factors in high-grade osteosarcoma of the extremities or trunk: an analysis of 1,702 patients treated on neoadjuvant cooperative osteosarcoma study group protocols. *J Clin Oncol.* 2002; 20:776–790.
4. Kager L, Zoubek A, Pötschger U, et al. Primary metastatic osteosarcoma: presentation and outcome of patients treated on neoadjuvant cooperative osteosarcoma study group protocols. *J Clin Oncol.* 2003;21:2011–2018.
5. Meyers PA, Schwartz CL, Krailo M, et al. Osteosarcoma: a randomized, prospective trial of the addition of ifosfamide and/or muramyl tripeptide to cisplatin, doxorubicin, and high-dose methotrexate. *J Clin Oncol.* 2005;23:2004–2011.
6. Partovi S, Kohan AA, Zipp L, et al. Hybrid PET/MR imaging in two sarcoma patients: clinical benefits and implications for future trials. *Int J Clin Exp Med.* 2014;7:640–648.
7. Behzadi AH, Raza SI, Carrino JA, et al. Applications of PET/CT and PET/MR imaging in primary bone malignancies. *PET Clin.* 2018;13:623–634.

8. Webb HR, Latifi HR, Griffeth LK. Utility of whole-body (head-to-toe) PET/CT in the evaluation of melanoma and sarcoma patients. *Nucl Med Commun.* 2018;39: 68–73.
9. London K, Stege C, Cross S, et al. ^{18}F-FDG PET/CT compared to conventional imaging modalities in pediatric primary bone tumors. *Pediatr Radiol.* 2012;42: 418–430.
10. Strobel K, Exner UE, Stumpe KD, et al. The additional value of CT images interpretation in the differential diagnosis of benign vs. malignant primary bone lesions with ^{18}F-FDG-PET/CT. *Eur J Nucl Med Mol Imaging.* 2008;35:2000–2008.
11. Quartuccio N, Fox J, Kuk D, et al. Pediatric bone sarcoma: diagnostic performance of ^{18}F-FDG PET/CT versus conventional imaging for initial staging and follow-up. *AJR.* 2015;204:153–160.
12. Franzius C, Sciuk J, Daldrup-Link HE, Jurgens H, Schober O. FDG-PET for detection of osseous metastases from malignant primary bone tumours: comparison with bone scintigraphy. *Eur J Nucl Med.* 2000;27:1305–1311.
13. Hurley C, McCarville MB, Shulkin BL, et al. Comparison of ^{18}F-FDG-PET-CT and bone scintigraphy for evaluation of osseous metastases in newly diagnosed and recurrent osteosarcoma. *Pediatr Blood Cancer.* 2016;63:1381–1386.
14. Byun BH, Kong CB, Lim I, et al. Comparison of ^{18}F-FDG PET/CT and ^{99m}Tc-MDP bone scintigraphy for detection of bone metastasis in osteosarcoma. *Skeletal Radiol.* 2013;42:1673–1681.
15. Liu F, Zhang Q, Zhou D, Dong J. Effectiveness of ^{18}F-FDG PET/CT in the diagnosis and staging of osteosarcoma: a meta-analysis of 26 studies. *BMC Cancer.* 2019; 19:323.
16. Carrle D, Bielack SS. Current strategies of chemotherapy in osteosarcoma. *Int Orthop.* 2006;30:445–451.
17. Geller DS, Gorlick R. Osteosarcoma: a review of diagnosis, management, and treatment strategies. *Clin Adv Hematol Oncol.* 2010;8:705–718.
18. Davis AM, Bell RS, Goodwin PJ. Prognostic factors in osteosarcoma: a critical review. *J Clin Oncol.* 1994;12:423–431.
19. Bishop MW, Chang Y-C, Krailo MD, et al. Assessing the prognostic significance of histologic response in osteosarcoma: a comparison of outcomes on CCG-782 and INT0133—a report from the Children's Oncology Group Bone Tumor Committee. *Pediatr Blood Cancer.* 2016;63:1737–1743.
20. Rosen G, Caparros B, Huvos AG, et al. Preoperative chemotherapy for osteogenic sarcoma: selection of postoperative adjuvant chemotherapy based on the response of the primary tumor to preoperative chemotherapy. *Cancer.* 1982;49:1221–1230.
21. Picci P, Bacci G, Campanacci M, et al. Histologic evaluation of necrosis in osteosarcoma induced by chemotherapy: regional mapping of viable and nonviable tumor. *Cancer.* 1985;56:1515–1521.
22. Salzer-Kuntschik M, Delling G, Beron G, Sigmund R. Morphological grades of regression in osteosarcoma after polychemotherapy: study COSS 80. *J Cancer Res Clin Oncol.* 1983;106:21–24.
23. Jones DN, McCowage GB, Sostman HD, et al. Monitoring of neoadjuvant therapy response of soft-tissue and musculoskeletal sarcoma using fluorine-18-FDG PET. *J Nucl Med.* 1996;37:1438–1444.
24. Benz MR, Czernin J, Tap WD, et al. FDG-PET/CT imaging predicts histopathologic treatment responses after neoadjuvant therapy in adult primary bone sarcomas. *Sarcoma.* 2010;2010:143540.
25. Cheon GJ, Kim MS, Lee JA, et al. Prediction model of chemotherapy response in osteosarcoma by ^{18}F-FDG PET and MRI. *J Nucl Med.* 2009;50:1435–1440.
26. Denecke T, Hundsdorfer P, Misch D, et al. Assessment of histological response of paediatric bone sarcomas using FDG PET in comparison to morphological volume measurement and standardized MRI parameters. *Eur J Nucl Med Mol Imaging.* 2010;37:1842–1853.
27. Hamada K, Tomita Y, Inoue A, et al. Evaluation of chemotherapy response in osteosarcoma with FDG-PET. *Ann Nucl Med.* 2009;23:89–95.
28. Kim DH, Kim SY, Lee HJ, et al. Assessment of chemotherapy response using FDG-PET in pediatric bone tumors: a single institution experience. *Cancer Res Treat.* 2011;43:170–175.
29. Kong CB, Byun BH, Lim I, et al. ^{18}F-FDG PET SUVmax as an indicator of histopathologic response after neoadjuvant chemotherapy in extremity osteosarcoma. *Eur J Nucl Med Mol Imaging.* 2013;40:728–736.
30. Nair N, Ali A, Green AA, et al. Response of osteosarcoma to chemotherapy: evaluation with F-18 FDG-PET scans. *Clin Positron Imaging.* 2000;3:79–83.
31. Schulte M, Brecht-Krauss D, Werner M, et al. Evaluation of neoadjuvant therapy response of osteogenic sarcoma using FDG PET. *J Nucl Med.* 1999;40: 1637–1643.
32. Ye Z, Zhu J, Tian M, et al. Response of osteogenic sarcoma to neoadjuvant therapy: evaluated by ^{18}F-FDG-PET. *Ann Nucl Med.* 2008;22:475–480.
33. Hawkins DS, Conrad EU III, Butrynski JE, Schuetze SM, Eary JF. [F-18]-fluorodeoxy-D-glucose-positron emission tomography response is associated with outcome for extremity osteosarcoma in children and young adults. *Cancer.* 2009;115: 3519–3525.
34. Huang TL, Liu RS, Chen TH, Chen WY, Hsu HC, Hsu YC. Comparison between F-18-FDG positron emission tomography and histology for the assessment of tumor necrosis rates in primary osteosarcoma. *J Chin Med Assoc.* 2006;69:372–376.
35. Byun BH, Kong CB, Lim I, et al. Combination of ^{18}F-FDG PET/CT and diffusion-weighted MR imaging as a predictor of histologic response to neoadjuvant chemotherapy: preliminary results in osteosarcoma. *J Nucl Med.* 2013;54:1053–1059.
36. Gaston LL, Di Bella C, Slavin J, Hicks RJ, Choong PF. ^{18}F-FDG PET response to neoadjuvant chemotherapy for Ewing sarcoma and osteosarcoma are different. *Skeletal Radiol.* 2011;40:1007–1015.
37. Im HJ, Kim TS, Park SY, et al. Prediction of tumour necrosis fractions using metabolic and volumetric ^{18}F-FDG PET/CT indices, after one course and at the completion of neoadjuvant chemotherapy, in children and young adults with osteosarcoma. *Eur J Nucl Med Mol Imaging.* 2012;39:39–49.
38. Davis JC, Daw NC, Navid F, et al. ^{18}F-FDG uptake during early adjuvant chemotherapy predicts histologic response in pediatric and young adult patients with osteosarcoma. *J Nucl Med.* 2018;59:25–30.
39. Hongtao L, Hui Z, Bingshun W, et al. ^{18}F-FDG positron emission tomography for the assessment of histological response to neoadjuvant chemotherapy in osteosarcomas: a meta-analysis. *Surg Oncol.* 2012;21:e165–e170.
40. Harrison DJ, Parisi MT, Khalatbari H, Shulkin BL. PET with ^{18}F-fluorodeoxyglucose/computed tomography in the management of pediatric sarcoma. *PET Clin.* 2020;15:333–347.
41. Byun BH, Kong CB, Lim I, et al. Early response monitoring to neoadjuvant chemotherapy in osteosarcoma using sequential ^{18}F-FDG PET/CT and MRI. *Eur J Nucl Med Mol Imaging.* 2014;41:1553–1562.
42. Im H-J, Bradshaw T, Solaiyappan M, Cho SY. Current methods to define metabolic tumor volume in positron emission tomography: which one is better? *Nucl Med Mol Imaging.* 2018;52:5–15.
43. Byun BH, Kim SH, Lim SM, et al. Prediction of response to neoadjuvant chemotherapy in osteosarcoma using dual-phase ^{18}F-FDG PET/CT. *Eur Radiol.* 2015;25: 2015–2024.
44. Im H-J, McIlwain S, Ong I, et al. Prediction of response to neoadjuvant chemotherapy using machine learning algorithm trained by baseline FDG-PET textural parameters in osteosarcoma [abstract]. *J Nucl Med.* 2017;58(suppl 1):44.
45. Kawai A, Healey JH, Boland PJ, Lin PP, Huvos AG, Meyers PA. Prognostic factors for patients with sarcomas of the pelvic bones. *Cancer.* 1998;82:851–859.
46. Ozaki T, Flege S, Liljenqvist U, et al. Osteosarcoma of the spine: experience of the Cooperative Osteosarcoma Study Group. *Cancer.* 2002;94:1069–1077.
47. Cates JMM. Simple staging system for osteosarcoma performs equivalently to the AJCC and MSTS systems. *J Orthop Res.* 2018;36:2802–2808.
48. Enneking WF, Kagan A. "Skip" metastases in osteosarcoma. *Cancer.* 1975;36: 2192–2205.
49. Testa S, Hu BD, Saadeh NL, et al. A retrospective comparative analysis of outcomes and prognostic factors in adult and pediatric patients with osteosarcoma. *Curr Oncol.* 2021;28:5304–5317.
50. Kelley LM, Schlegel M, Hecker-Nolting S, et al. Pathological fracture and prognosis of high-grade osteosarcoma of the extremities: an analysis of 2,847 consecutive cooperative osteosarcoma study group (COSS) patients. *J Clin Oncol.* 2020;38: 823–833.
51. Costelloe CM, Macapinlac HA, Madewell JE, et al. ^{18}F-FDG PET/CT as an indicator of progression-free and overall survival in osteosarcoma. *J Nucl Med.* 2009;50: 340–347.
52. Byun BH, Kong CB, Park J, et al. Initial metabolic tumor volume measured by ^{18}F-FDG PET/CT can predict the outcome of osteosarcoma of the extremities. *J Nucl Med.* 2013;54:1725–1732.
53. Bailly C, Leforestier R, Campion L, et al. Prognostic value of FDG-PET indices for the assessment of histological response to neoadjuvant chemotherapy and outcome in pediatric patients with Ewing sarcoma and osteosarcoma. *PLoS One.* 2017;12:e0183841.
54. Im HJ, Zhang Y, Wu H, et al. Prognostic value of metabolic and volumetric parameters of FDG PET in pediatric osteosarcoma: a hypothesis-generating study. *Radiology.* 2018;287:303–312.
55. Angelini A, Ceci F, Castellucci P, et al. The role of ^{18}F-FDG PET/CT in the detection of osteosarcoma recurrence. *Eur J Nucl Med Mol Imaging.* 2017;44: 1712–1720.
56. Sharp SE, Shulkin BL, Gelfand MJ, McCarville MB. FDG PET/CT appearance of local osteosarcoma recurrences in pediatric patients. *Pediatr Radiol.* 2017;47: 1800–1808.
57. Purz S, Sabri O, Viehweger A, et al. Potential pediatric applications of PET/MR. *J Nucl Med.* 2014;55(suppl 2):32S–39S.
58. Manhas NS, Salehi S, Joyce P, Guermazi A, Ahmadzadehfar H, Gholamrezanezhad A. PET/computed tomography scans and PET/MR imaging in the diagnosis and management of musculoskeletal diseases. *PET Clin.* 2020;15:535–545.

59. Schäfer JF, Gatidis S, Schmidt H, et al. Simultaneous whole-body PET/MR imaging in comparison to PET/CT in pediatric oncology: initial results. *Radiology.* 2014;273:220–231.
60. Platzek I, Beuthien-Baumann B, Schramm G, et al. FDG PET/MR in initial staging of sarcoma: initial experience and comparison with conventional imaging. *Clin Imaging.* 2017;42:126–132.
61. Eiber M, Takei T, Souvatzoglou M, et al. Performance of whole-body integrated ^{18}F-FDG PET/MR in comparison to PET/CT for evaluation of malignant bone lesions. *J Nucl Med.* 2014;55:191–197.
62. Buchbender C, Heusner TA, Lauenstein TC, Bockisch A, Antoch G. Oncologic PET/MRI, part 2: bone tumors, soft-tissue tumors, melanoma, and lymphoma. *J Nucl Med.* 2012;53:1244–1252.
63. Orsatti G, Zucchetta P, Varotto A, et al. Volumetric histograms-based analysis of apparent diffusion coefficients and standard uptake values for the assessment of pediatric sarcoma at staging: preliminary results of a PET/MRI study. *Radiol Med (Torino).* 2021;126:878–885.
64. Theruvath AJ, Siedek F, Muehe AM, et al. Therapy response assessment of pediatric tumors with whole-body diffusion-weighted MRI and FDG PET/MRI. *Radiology.* 2020;296:143–151.
65. Baratto L, Hawk KE, States L, et al. PET/MRI improves management of children with cancer. *J Nucl Med.* 2021;62:1334–1340.
66. Bastawrous S, Bhargava P, Behnia F, Djang DS, Haseley DR. Newer PET application with an old tracer: role of ^{18}F-NaF skeletal PET/CT in oncologic practice. *Radiographics.* 2014;34:1295–1316.
67. Chou YH, Ko KY, Cheng MF, Chen WW, Yen RF. ^{18}F-NaF PET/CT images of cardiac metastasis from osteosarcoma. *Clin Nucl Med.* 2016;41:708–709.
68. Cai L, Chen Y, Huang Z, Wu J. Incidental detection of solitary hepatic metastasis by ^{99m}Tc-MDP and ^{18}F-NaF PET/CT in a patient with osteosarcoma of the tibia. *Clin Nucl Med.* 2015;40:759–761.
69. Verma P, Purandare N, Agrawal A, Shah S, Rangarajan V. Unusual finding of a tumor thrombus arising from osteosarcoma detected on ^{18}F-NaF PET/CT. *Clin Nucl Med.* 2016;41:e304–e306.
70. Kairemo K, Rohren EM, Anderson PM, et al. Development of sodium fluoride PET response criteria for solid tumours (NAFCIST) in a clinical trial of radium-223 in osteosarcoma: from RECIST to PERCIST to NAFCIST. *ESMO Open.* 2019;4:e000439.
71. Kratochwil C, Flechsig P, Lindner T, et al. ^{68}Ga-FAPI PET/CT: tracer uptake in 28 different kinds of cancer. *J Nucl Med.* 2019;60:801–805.
72. Koerber SA, Finck R, Dendl K, et al. Novel FAP ligands enable improved imaging contrast in sarcoma patients due to FAPI-PET/CT. *Eur J Nucl Med Mol Imaging.* 2021;48:3918–3924.
73. Kessler L, Ferdinandus J, Hirmas N, et al. ^{68}Ga-FAPI as a diagnostic tool in sarcoma: data from the ^{68}Ga-FAPI PET prospective observational trial. *J Nucl Med.* 2022;63:89–95.
74. Zhao L, Chen J, Pang Y, et al. Fibroblast activation protein-based theranostics in cancer research: a state-of-the-art review. *Theranostics.* 2022;12:1557–1569.
75. Butch ER, Mead PE, Amador Diaz V, et al. Positron emission tomography detects in vivo expression of disialoganglioside GD2 in mouse models of primary and metastatic osteosarcoma. *Cancer Res.* 2019;79:3112–3124.
76. Trautwein NF, Reischl G, Seitz C, et al. First-in-humans PET/MRI of in vivo GD2 expression in osteosarcoma. *J Nucl Med.* 2023;64:337–338.